Plasticity in Ca^{2+} selectivity of Orai1/Orai3 heteromeric channel

Rainer Schindl[a,1,2], Irene Frischauf[a,2], Judith Bergsmann[a,2], Martin Muik[a], Isabella Derler[a], Barbara Lackner[a], Klaus Groschner[b], and Christoph Romanin[a,1]

[a]Institute of Biophysics, University of Linz, A-4040 Linz, Austria; and [b]Department of Pharmaceutical Technology, University of Graz, A-8010 Graz, Austria

Edited by Anjana Rao, Harvard Medical School, Boston, MA, and approved September 30, 2009 (received for review July 10, 2009)

A general cellular response following depletion of intracellular calcium stores involves activation of store-operated channels (SOCs). While Orai1 forms the native Ca^{2+} release-activated Ca^{2+} (CRAC) channel in mast and T cells, the molecular architecture of less Ca^{2+} selective SOCs is insufficiently defined. Here we present evidence that diminished Ca^{2+} selectivity and robust Cs^{+} permeation together with a reduced fast inactivation are characteristics of heteromeric Orai1 and Orai3 channels in contrast to their homomeric forms. The first extracellular loop of these Orai isoforms differs by two aspartates replacing glutamates that affect the selectivity. Co-expression of an Orai3 mutant that mimicked the first loop of Orai1 with either Orai1 or Orai3 recovered or decreased Ca^{2+} selectivity, respectively. Heteromeric Orai1/3 protein assembly provides a concept for less Ca^{2+}-selective SOCs.

heteromer | SOC

Store-operated calcium entry is an ubiquitous mechanism for refilling internal Ca^{2+} stores in many cells (1). Upon store depletion, the endoplasmic reticulum resident Ca^{2+} sensor Stim1 multimerizes, redistributes and activates the three Orai channels (also termed CRACM) in the plasma membrane leading to highly Ca^{2+}-selective currents (2–5). Orai1 is strongly expressed in lymphoid organs, skeletal muscle, liver, and skin (6, 7). While Orai3 is detected in similar tissues as Orai1, Orai2 is predominantly found in murine brain (8) or human kidney, lung, and spleen (9). T-cells of patients with a severe combined immunodeficiency lacked CRAC currents due to non-functional Orai1 channels, caused by a single point mutation (6, 10–12). In line, Orai1 deficiency in mice impaired Ca^{2+} influx and cytokine production in T cells (6), degranulation in mast cells (7), and thrombus formation of platelets (13, 14). Store-operated channels (SOCs) observed in various cell types such as endothelial, smooth muscle, or epidermal cells differ in Ca^{2+} selectivity and cation permeability (1). These SOCs have been reported to include members of canonical transient receptor potentials probably in combination with Orai1 (15–17). Orai3 might represent an additional candidate for native SOCs when co-expressed with Orai1 in hepatocytes (18), airway smooth muscle cells (19), and myoblasts (20), although clear demonstration of formation of native heteromeric Orai1/Orai3 channels that additionally show a reduced Ca^{2+} selectivity is so far missing.

Results and Discussion

The capability of heteromeric Orai assembly has been demonstrated biochemically (9, 21, 22). We initially evaluated the potential of Orai1 and Orai3 heteromerization by employing fluorescence resonance energy transfer (FRET) microscopy. Both, N-terminally labeled CFP-Orai1 (Fig. 1*A*, first image) and YFP-Orai3 (Fig. 1*A*, second image) overexpressed in human embryonic kidney (HEK) cells 293 cells exhibited clear plasma-membrane targeting and extensive colocalization (Fig. 1*A*, third image) in correlation with robust calculated FRET values (Fig. 1*A*, fourth image). In comparison, homomeric CFP-/YFP-Orai3 co-expression yielded even higher FRET (Fig. 1 *B* and *C*), while homomeric Orai1 oligomerization (5) exhibited significantly lower FRET than Orai1/Orai3 (Fig. 1*C*).

Both, Orai1 and Orai3, each individually co-expressed with Stim1 displayed store-operated, highly Ca^{2+}-selective inward currents that reversed at a similar range of $+58 \pm 3$ mV ($n = 10$ cells) and $+56 \pm 5$ mV ($n = 10$ cells), respectively. In an attempt to characterize heteromeric Orai1/3 currents we overexpressed Stim1-mCherry together with CFP-Orai1 and YFP-Orai3. Store-operated currents were activated by passive store-depletion with 10 mM EGTA added to the pipette solution in a 10 mM Ca^{2+} containing bath solution as shown in the time-course at -84 and $+62$ mV (Fig. 1*D*). Interestingly, current-voltage relationship of Stim1, Orai1, and Orai3 expressing cells exhibited not only a prominent inward rectification but also small yet significant outward currents resulting in an average reversal potential of $+33 \pm 7$ mV (Fig. 1*E*, $n = 11$ cells). We supposed that the outward component derived from Orai1 and Orai3 co-expression was mainly mediated by Cs^{+}, which represented the main cation in the pipette solution. Indeed, perfusion with a Cs^{+}-based divalent free solution (Cs^{+}-DVF), after Ca^{2+} currents had been fully developed, resulted in an increase in inward currents that reversed at -2 ± 2 mV ($n = 11$ cells) as expected for Cs^{+}-based bath and pipette solutions (Fig. 1*E*). In contrast, store-operated Orai3 (*23*) as well as Orai1 (Fig. 1 *F* and *G*) Ca^{2+} currents were largely reduced by perfusion with a Cs^{+}-DVF solution.

The narrowest part of the Orai1 and Orai3 pore is approximately 3.8 Å (23, 24), suggesting that steric hindrance most likely accounts for low Cs^{+} permeability in homomeric Orai channels. Therefore, increased Cs^{+} permeability and consequently reduced Ca^{2+} selectivity is a fingerprint of the heteromeric assembly of Orai1 and Orai3 proteins.

In contrast to Cs^{+}, both homomeric Orai1 (Fig. 1*H*), as well as Orai3 channels (24) are permeable to sodium in a DVF solution (Na^{+}-DVF), yielding an inward rectifying current-voltage relationship that reversed at $+43 \pm 3$ mV ($n = 6$ cells) and $+46 \pm 5$ mV ($n = 4$ cells), respectively. Co-expression of Orai1 and Orai3 together with Stim1 led to an inward rectifying current-voltage relationship in Na^{+}-DVF solution with a remaining outward component that reversed at $+32 \pm 7$ mV (Fig. 1*I*; $n = 5$ cells). This leftward shift compared to homomeric Orai channels reflected an increase in relative Cs^{+} permeability.

Functional Orai channels have been demonstrated to form tetramers (25, 26) and are capable of heteromerization. The above described co-expression of Orai1 and Orai3 probably resulted in a repertoire of possible heteromeric but also homomeric channels with functionally overlapping currents. A heteromeric Orai1/Orai3 channel has also been reported to form arachidonate-regulated

Author contributions: R.S. and C.R. designed research; R.S., I.F., J.B., M.M., I.D., and B.L. performed research; I.F. and J.B. contributed new reagents/analytic tools; R.S., M.M., I.D., B.L., K.G., and C.R. analyzed data; and R.S. and C.R. wrote the paper.

The authors declare no conflict of interest.

This article is a PNAS Direct Submission.

[1]To whom correspondence may be addressed. E-mail: rainer.schindl@jku.at or christoph.romanin@jku.at.

[2]R.S., I.F., and J.B. contributed equally to this work.

This article contains supporting information online at www.pnas.org/cgi/content/full/0907714106/DCSupplemental.

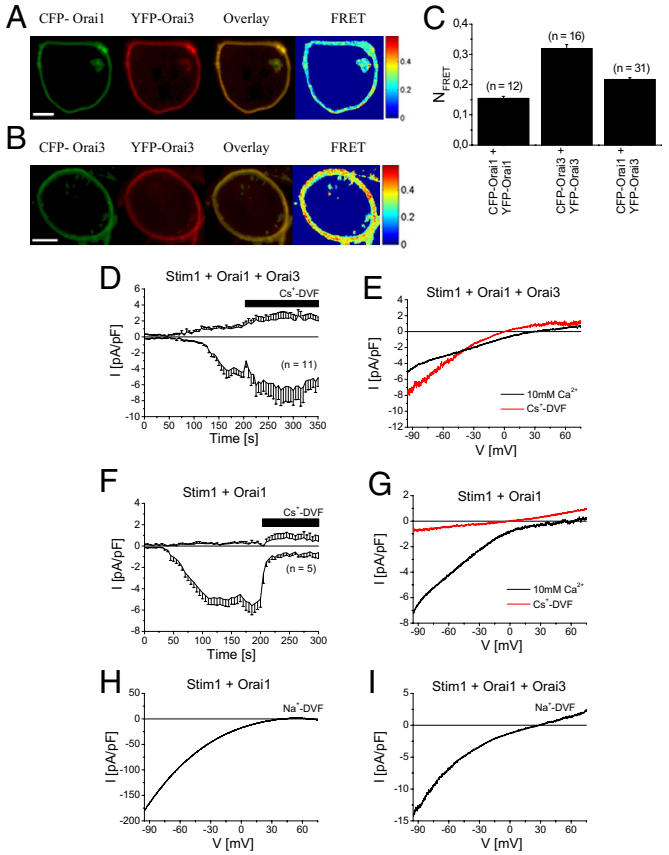

Fig. 1. Orai1 and Orai3 co-expression exhibits reduced Ca^{2+} selectivity. (*A*) Fluorescence images from a representative cell co-expressing CFP-Orai1 and YFP-Orai3 or (*B*) CFP-/YFP-Orai3, overlay and calculated FRET. (*C*) Average FRET values determined for the constructs shown in (*A* and *B*) and CFP-/YFP-Orai1. (*D*) Time course of whole-cell currents at −86 mV and +62 mV of HEK cells overexpressing Stim1, Orai1, and Orai3 or (*F*) Stim1 and Orai1 are monitored upon passive store-depletion by 10 mM EGTA in a 10 mM Ca^{2+} bath solution followed by perfusion of a Cs^+ based divalent free solution (Cs^+-DVF) after 200 s. (*E*) Corresponding representative current voltage relationships were taken from voltage ramps in both a Ca^{2+} and Cs^+ containing bath solution for Stim1, Orai1, and Orai3 expressing cells or (*G*) Stim1 and Orai1 co-expression. (*H*) IV characteristic for Na^+-DVF solution for Stim1 and Orai1 or (*I*) Stim1, Orai1, and Orai3 overexpression.

(ARC) channels, yet with a high Ca^{2+}-selectivity (27). In an attempt to markedly promote the formation of Orai1/Orai3 heteromers with 1:1 stoichiometry, we generated a tandem construct where Orai3 is linked C-terminally to the N terminus of Orai1 (Orai3-Orai1). This Orai3-Orai1 tandem was clearly targeted to the plasma-membrane (Fig. 2*A*) and exhibited robust homomeric FRET (N_{FRET} = 0,16 ± 0,01; n = 16 cells) consistent with the formation of tetrameric assemblies. Moreover, passive store-depletion of Stim1 and Orai3-Orai1 tandem expressing HEK cells activated inwardly rectifying currents with significant outward currents and a current-voltage relationship that reversed at +26 ± 4 mV (Fig. 2 *B* and *C*, n = 18 cells). It is of note, however, that more positive reversal potentials have been recently reported from tetrameric concatamers of various Orai1/Orai3 stoichiometries activated either by arachidonic acid or by store depletion (28). The reason for the different results is so far unclear. Nonetheless, the authors of this report have indicated (28) that experiments displaying outward currents at +60 mV are excluded from analysis. When Ca^{2+} containing extracellular solutions were exchanged by Cs^+-DVF ones after complete store-operated activation, inward currents robustly increased about 4-fold, underlining Cs^+-permeation as a fingerprint of heteromeric Orai1/Orai3 currents (Fig. 2 *B* and *D*; V_{rev} = −2 ± 2 mV, n = 9 cells). In a similar approach, perfusion with a Na^+-DVF also resulted in an increase in inward currents and a reversal potential of +7 ± 2 mV (Fig. 2 *E* and *F*; n = 10 cells). With an estimated permeability ratio P_{Cs}/P_{Na} = 0.73 ± 0.07 calculated by the Goldman-Hodgkin-Katz equation (29), the Orai3-Orai1 tandem is dramatically less selective for Na^+ over Cs^+ under divalent-free conditions in comparison to 0.18 ± 0.02 for Orai1 and 0.11 ± 0.02 for Orai3 in line with a previous calculation of 0.15 for Orai1 currents (*24*). Native CRAC channels (30) in Jurkat T-cells yielded P_{Cs}/P_{Na} = 0.13. In comparison to the co-expression of separate Orai1 and Orai3 constructs, the current properties derived from the tandem Orai3-Orai1 pointed to even lower Na^+ over Cs^+ selectivity, probably due to the lack of overlapping homomeric Orai channels.

The high Ca^{2+} selectivity of homomeric Orai1 and Orai3 currents was additionally demonstrated by replacing Na^+ in the bath solution with impermeable tetraethylammonium (TEA^+), thereby leaving Ca^{2+} as solely permeable cation (31). Fully activated Orai1 currents were slightly, but not significantly increased, while Orai3 currents were unaffected in this solution (Fig. 2*G*). In contrast Orai3-Orai1 tandem mediated currents were significantly reduced by 30% in the Ca^{2+}/TEA^+ solution within 25 s (Fig. 2*G*), revealing that these less-Ca^{2+}-selective currents carried a substantial amount of Na^+. Beside decreased inward currents, also outward currents of Orai3-Orai1 tandem were slightly attenuated, concomitant with a rightward shift in reversal potential. It is likely that a solely Ca^{2+}-mediated influx stabilized Ca^{2+} binding at the pore entrance and resulted in diminished outward currents as well as an increase in Ca^{2+} selectivity. Furthermore we investigated how heteromeric Orai1/Orai3 currents behaved in a more physiological environment of a 145 mM K^+ intracellular solution. Therefore Cs^+ was substituted by K^+ in the pipette solution and 10 mM TEA^+ was added to the bath side to inhibit endogenously expressed K^+ channels (31). Co-expression of Stim1 with either Orai1 or Orai3 resulted in store-depletion activated Ca^{2+} currents that yielded a reversal potential of 51.2 ± 6.6 mV (n = 11 cells) and 49.4 ± 3.7 mV (n = 8 cells; Fig. 2 *H* and *I*), respectively. Stim1 with Orai3-Orai1 tandem co-expressing cells yielded Ca^{2+} currents with a significant outward current that reversed at 22.7 ± 5.2 mV (n = 9 cells). The respective reversal potentials for Orai1, Orai3, and Orai1-Orai3 tandem were leftward shifted, yet not significantly different ($P > 0.05$) to those obtained with the Cs^+ pipette solution.

A physiological difference of endogenous CRAC, Orai1 and Orai3 currents are their inactivation characteristics (*22*), while those of Orai1 can be additionally modulated by Stim1 expression levels (32). A well characterized, physiological feedback mechanism for CRAC currents is their robust Ca^{2+}-dependent fast inactivation within the first 100 ms due to elevated Ca^{2+} concentrations within a microdomain close to the channel mouth (33–35).

Following store-operated activation of Orai currents, step protocols from a holding potential of 0 to −100 mV up to −40 mV for 2 s were used to investigate current inactivation. In line with previous results (*22*) we observed for Stim1 and Orai1 expressing cells an initial moderate phase of fast inactivation at −80 and −100 mV within the first 100 ms followed by a slow reactivation (Fig. 3 *A*, *D*, and *E*). In contrast co-expression of Stim1 and Orai3 yielded a pronounced inactivation, while only at −100 mV a slight reactivating phase was visible (Fig. 3 *B*, *D*, and *E*). Normalized inactivation profiles at −80 mV were displayed for homo- and heteromeric Orai1 and Orai3 currents in Fig. 3 *D* and *E*. Interestingly, Orai3-Orai1 tandem did not display a mean inactivation of Orai1 and Orai3, but was closer to the reduced fast inactivation of wild-type Orai1 currents (Fig. 3 *C* and *E*) while lacking the second phase of reactivation except at a potential of −100 mV. In line, Yamashita et al. (24) have shown that Orai1 pore mutants that are less Ca^{2+} selective develop a reduced Ca^{2+}-dependent fast inactivation.

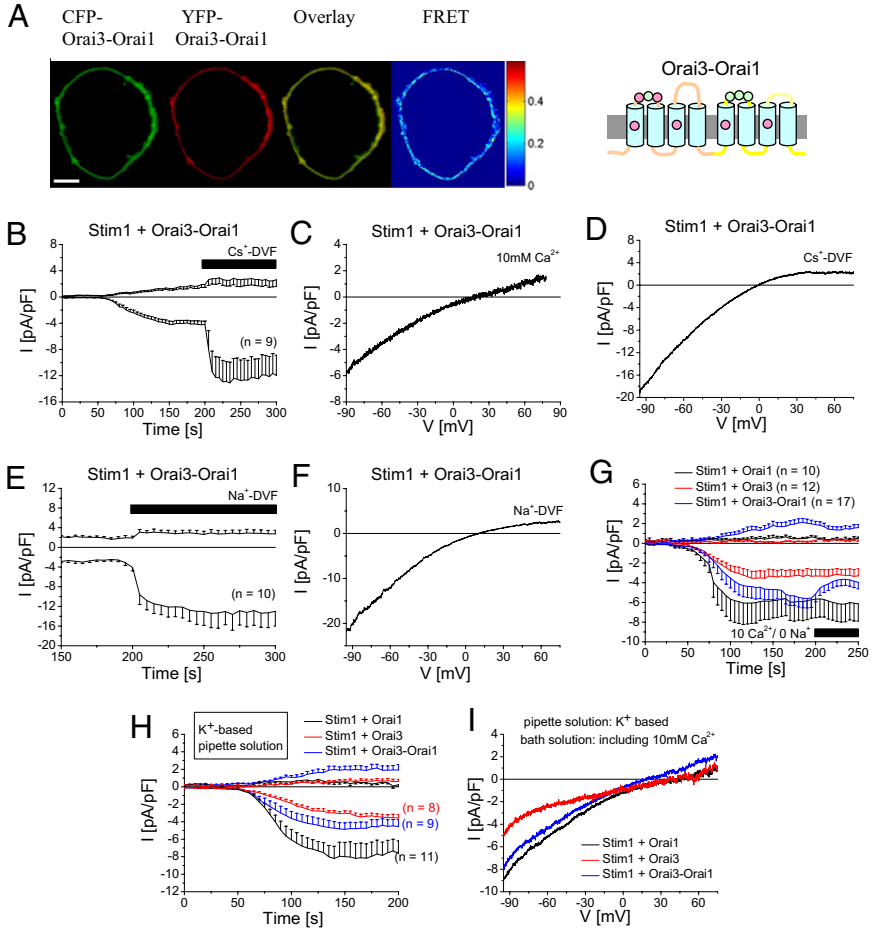

Fig. 2. Permeation properties of Orai3-Orai1 tandem. (*A*) Localization, overlay and FRET of CFP-/YFP-Orai3-Orai1. (*B*) Time course of Stim1 and Orai3-Orai1 co-expression depicting activation of Ca^{2+} currents upon passive store-depletion, followed by perfusion of a Cs^{+}-DVF solution after 200 s. Corresponding representative current voltage relationships were taken from voltage ramps in a (*C*) 10 mM Ca^{2+}, (*D*) Cs^{+}-DVF, or (*F*) Na^{+}–DVF containing bath solution for Stim1 and Orai3-Orai1 expressing cells. (*E*) Fully activated Ca^{2+} currents of Stim1 and Orai3-Orai1 co-expression are followed by Na^{+}-DVF solution. (*G*) Ca^{2+} current of Stim1 co-expressed with either Orai1, Orai3 or Orai3-Orai1 were activation by store-depletion and Na^{+} and Cs^{+} was substituted by TEA^{+} in the bath solution after 200 s. (*H*) Time course of currents and (*I*) current-voltage relationship of a co-expression of STIM1 with either Orai1, Orai3, or Orai3-Orai1 activated by a 10 mM EGTA and K^{+}-based pipette solution.

Therefore, heteromeric Orai1/Orai3 channels attained an inactivation profile that led to a Ca^{2+}-feedback regulation.

Another striking difference between homomeric Orai channels is based on the pharmacological action of the drug 2-aminoethoxydiphenyl borate (2-APB). While 5–10 μM 2-APB enhance inward-currents of Orai1, increasing concentrations inhibit them (3). In contrast 2-APB solely augments the Orai3 current and leads to a double-rectifying current-voltage relationship and a wider pore radius (23). After full Orai3-Orai1 tandem current activation in the presence of Stim1, addition of 75 μM 2-APB resulted in a transient stimulation of inward currents (Fig. 3 *F* and *G*) that was followed only by a slight current reduction (Fig. 3*F*) concomitant with a change to a double-rectifying current-voltage relationship (Fig. 3*G*). The initial 2-APB induced small, transient increase in inward currents was dependent on Stim1, as Orai3-Orai1 tandem currents in the absence of Stim1 lacked it (Fig. 3*F*). Moreover, unique characteristics of the 2-APB evoked Orai3-Orai1 double-rectifying currents were their slower activation and the similar size of inward and outward currents (Fig. 3*F*) in contrast to a faster 2-APB response and larger outward than inward currents of co-expressed Orai3 and Orai1 (Fig. 3*H*). Furthermore, Orai3 and Orai1 together with Stim1 responded to 2-APB by a substantial increase in inward currents (Fig. 3*H*) most likely due to a remaining amount of homomeric Orai3 channels that are not assembled to an Orai1/Orai3 heteromer. Accordingly, Orai3 inward currents are typically 10-fold stimulated by 2-APB (23), while Orai3-Orai1 tandem currents after the transient increase were reduced by about 40% as compared to maximum store-operated ones underscoring the unique 2-APB profile obtained with Orai3-Orai1 tandem.

We assumed that the heteromeric Orai1/Orai3 permeation properties are based on alterations of the pore. Amino acids that contribute to the putative selectivity filter have been derived from mutagenesis for both Orai1 (12, 31) and Orai3 (23) and include fully conserved glutamates within the transmembrane (TM) domains one and three. The non-conserved glutamates and aspartates in the adjacent, first extracellular loop might also affect the selectivity profile (31). While Orai1 contains three aspartates within this loop (D110, D112, and D114), the corresponding Orai3 loop comprises of glutamates and aspartates (E85, D87, and E89). It is tempting to speculate that in a heteromeric Orai1/Orai3 channel, aspartates and glutamates come in close proximity, for example, D110 in Orai1 and E85 in Orai3. Thus a non-symmetric amino acid configuration in contrast to that of homomeric Orai1 or Orai3 channels might result in altered pore conformation thereby allowing for increased Cs^{+} permeability and reduced Ca^{2+} selectivity.

To mimic the critical amino acids within the first loop of Orai1 in Orai3 proteins, we mutated both glutamates in Orai3 loop domain to aspartates (Orai3-E85D-E89D). Co-expression of YFP-Orai3-E85D-E89D with either CFP-Orai1 or CFP-Orai3 resulted in their plasma-membrane expression and in a similar robust FRET as obtained with wild-type YFP-Orai3 (Fig. S1 *a*, *b*, and *g*). Passive store-depletion of Stim1 and Orai3-E85D-E89D co-expressing cells resulted in activation of highly Ca^{2+} selective inward-rectifying currents (Fig. 4 *B* and *H*), which were markedly diminished in a Cs^{+}-DVF solution, similar to homomeric wild-type Orai channels (Fig. 4*A*). Analogously, co-expression of Stim1, Orai1 and Orai3-E85D-E89D, simulating the homomeric Orai1 selectivity filter, resulted in activation of Ca^{2+} selective currents (Fig. 4 *C*, *D*, and *H*). Upon Cs^{+}-DVF perfusion, currents were diminished, yet remained

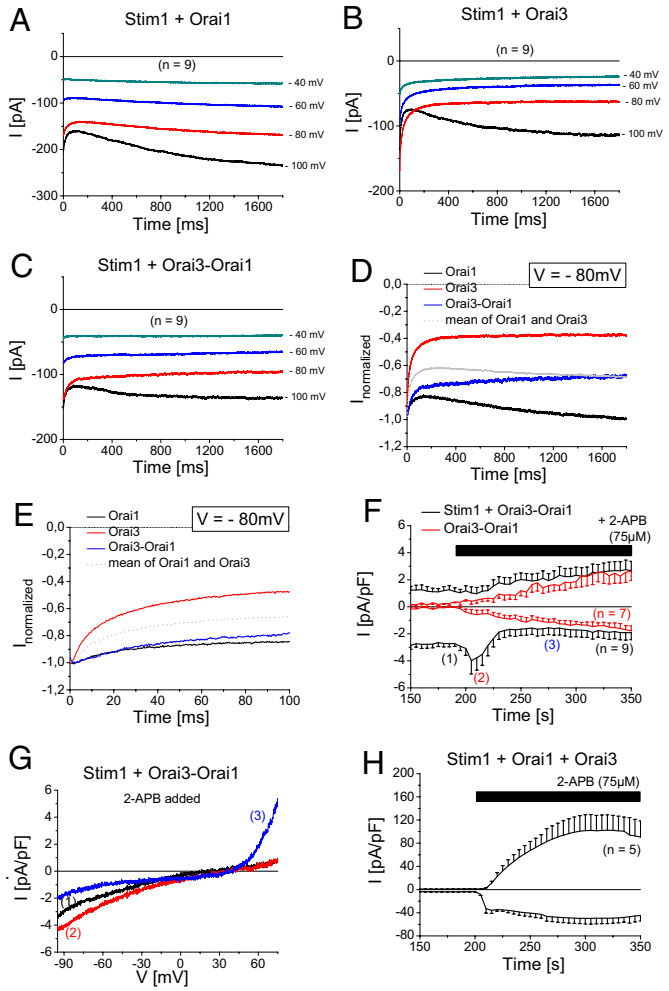

Fig. 3. Unique Ca^{2+} feedback regulation and 2-APB response of Orai3-Orai1 tandem. (*A–C*) Voltage steps from a holding potential of 0mV to −100, −80, −60, and −40 mV are depicted for a co-expression of Stim1 with either (*A*) Orai1, (*B*) Orai3, or (*C*) Orai3-Orai1 upon full store-depletion. (*D* and *E*) Normalized voltage step to −80 mV are shown for a co-expression of Stim1 with Orai1, Orai3, or Orai3-Orai1 over (*D*) 1,800 ms or (*E*) 100 ms. (*F*) Time course of fully activated Ca^{2+} currents of Stim1 and Orai3-Orai1 co-expression or solely expressing Orai3-Orai1 cells (in red) followed by addition of 75 μM 2-APB at 200 s. (*G*) IV characteristic for Stim1 and Orai3-Orai1 co-expression at depicted time-points (1) for maximum store-operated Ca^{2+} currents, (2) 5 s, and (3) 80 s after addition of 2-APB (75 μM). (*H*) Time course of of fully activated Ca^{2+} currents of Stim1, Orai1, and Orai3 expression following addition of 75 μM 2-APB at 200 s

slightly larger than in homomeric Orai channels. In contrast, co-expression of Stim1 with Orai3 and Orai3-E85D-E89D resulted in store-operated inward-rectifying Ca^{2+} currents with a small outward current and reversed significantly left shifted (Fig. 4 *E*, *F*, and *H*). Perfusion with Cs^+-DVF solution increased both inward as well as outward currents, resembling permeation characteristics of heteromeric Orai1/Orai3 currents (Fig. 4 *E*, *F*, and *H*). Co-expression of Orai3-E85D-E89D together with Stim1 led in Na^+-DVF solution to an inward rectifying current-voltage relationship (Fig. 4 *G* and *H*) with characteristics similar to co-expression of Stim1, Orai1 and Orai3-E85D-E89D (Fig. 4 *G* and *H*). However, Stim1, Orai3, and Orai3-E85D-E89D derived currents showed a significantly left-shifted reversal potential with an increased P_{Cs+}/P_{Na^+} ratio (Fig. 4 *G* and *H*) consistent with the increased Cs^+ currents. These experiments highlighted the significance of the asymmetric loop regions for reduced Ca^{2+} selectivity and increased Cs^+ permeability.

In a next step, we investigated if single glutamate to aspartate substitutions (Orai3-E85D; Orai3-E89D) were already sufficient to alter Ca^{2+} and Cs^+ permeation. In fluorescence microscopy experiments, either YFP-Orai3-E85D or YFP-Orai3-E89D co-expressed with either CFP-Orai1 or CFP-Orai3 resulted in robust FRET in the plasma-membrane (Fig. S1 *c–g*) similar to wild-type Orai3. Store-dependent activation of Orai3-E85D (Fig. S2 *a* and *b*) as well as Orai3-E89D (Fig. S2 *d* and *e*) resulted in highly Ca^{2+} selective inward-rectifying Ca^{2+} currents that were diminished by Cs^+-DVF solution (Fig. S3*i*).

Co-expression of Stim1, Orai1 and Orai3-E85D yielded store-operated inward-rectifying currents (Fig. S3 *a*, *b*, and *i*). Perfusion of Cs^+-DVF solution following full activation, decreased inward currents about 2.3-fold, yet Cs^+-currents remained clearly visible (Fig. S3 *a*, *b*, and *i*). In comparison, co-expression of Stim1, Orai3 and Orai3-E85D yielded store-operated Ca^{2+} currents with a leftward shifted reversal potential (Fig. S3 *c*, *d*, and *i*). Concomitant with a reduced Ca^{2+} selectivity, Cs^+-DVF solution resulted in an increase in both inward and outward currents (Fig. S3 *c*, *d*, and *i*). In a Na^+-DVF solution, Stim1 and Orai3-E85D co-expression resulted in inward currents with a high reversal potential (Fig. S3*i* and Fig. S2*c*), which was left-shifted for Stim1 and Orai3-E85D co-expressed with either Orai1 or Orai3 (Fig. 3*I* and Fig. S2*c*) in parallel to an increase in P_{Cs}/P_{Na}.

In an analogous approach we also co-expressed Orai3-E89D with both Orai1 and Stim1, yielding store-operated inward-rectifying Ca^{2+} currents (Fig. S3 *e*, *f*, and *i*). Exchanging bath solution by a Cs^+-DVF one, led to a comparable current size yet with a left-shifted reversal potential (Fig. S3 *e* and *f*). Co-expression of Orai3-E89D with Orai3 and Stim1 resulted in high Ca^{2+} selectivity and robustly suppressed Cs^+ currents (Fig. S3 *g–i*). In a Na^+-DVF solution, Stim1 and Orai3-E89D co-expressing cells yielded inward currents with a similar high reversal potential and a low P_{Cs}/P_{Na} as those of Stim1, Orai3 and Orai3-E89D (Fig. S3*i* and Fig. S2*c*). In contrast Stim1, Orai1, and Orai3-E89D currents yielded a lower reversal potential together with an increased P_{Cs}/P_{Na} (Fig. S3*i* and Fig. S2*f*).

Hence, an asymmetric arrangement of aspartate/glutamate within the first loops as generated by a heteromer of Orai3-E85D and wild-type Orai3 is most effective in altering selectivity. A similar asymmetry induced by combination of wild-type Orai1 and Orai3-E89D also enabled partial Cs^+ permeation yet displaying a higher Ca^{2+} reversal potential.

According to a model introduced by the groups of Penner and Kinet (31), the glutamates within the transmembrane domain one and three, as well as aspartates and glutamates in the first loop may form a negatively charged ring that coordinate binding of Ca^{2+} ions. In a heteromeric Orai1/Orai3 channel the selectivity filter located in TM1 and 3 is preserved with glutamates, while the first and the third negatively charged amino acids in the first loop are either an aspartate or glutamate, respectively. Within the first loop these amino acids are not only in close contact to each other but are assumedly in the vicinity to corresponding sites of the other subunits within a tetrameric channel. Thus, the distinct side-chain lengths of the non-conserved glutamates and aspartates within the heteromeric channel are expected to alter their orientation or localization thereby resulting in an overall asymmetric arrangement. We therefore suggest that this asymmetric domain contributes to the selectivity profile, resulting in reduced Ca^{2+} selectivity. In homomeric Orai channels Cs^+ influx is sterically hindered, as the minimum pore size of 3.8 Å would in principal allow Cs^+ permeation (*23*, *24*). In one scenario, a decreased potential of this asymmetric domain for binding extracellular Ca^{2+} ions may lead to a reduced occupancy of Ca^{2+} ions in the pore thus decreasing the barrier for outward currents. Alternatively, the orientation or localization of the distinct side chains of glutamates and aspartates in Orai1/Orai3 heteromer, via an allosteric mechanism, might lead to a distortion of the narrow pore region in the vicinity of the selectivity filter

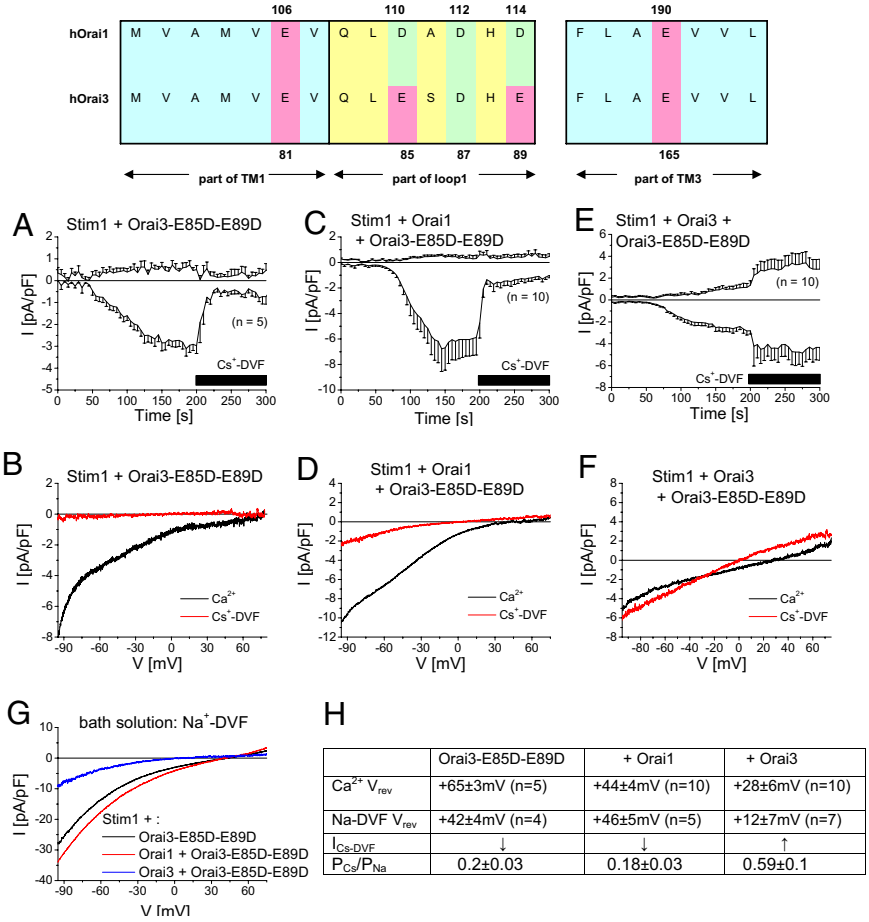

H

	Orai3-E85D-E89D	+ Orai1	+ Orai3
Ca^{2+} V_{rev}	+65±3mV (n=5)	+44±4mV (n=10)	+28±6mV (n=10)
Na-DVF V_{rev}	+42±4mV (n=4)	+46±5mV (n=5)	+12±7mV (n=7)
$I_{Cs\text{-}DVF}$	↓	↓	↑
P_{Cs}/P_{Na}	0.2±0.03	0.18±0.03	0.59±0.1

Fig. 4. Asymmetry of aspartates and glutamates in Orai1 and Orai3 first loop determines Ca^{2+} selectivity and Cs^{+} permeability. Upper panel, amino acid sequence of the first and third transmembrane domain and the first loop of both Orai1 and Orai3 including glutamates (red) and aspartates (green) that affect permeability. Time course of HEK cells co-expressing (*A*) Stim1 and Orai3-E85D-E89D, (*C*) Stim1, Orai1 and Orai3-E85D-E89D, or (*E*) Stim1, Orai3, and Orai3-E85D-E89D showing activation of Ca^{2+} currents upon passive store-depletion, followed by perfusion of a Cs^{+}-DVF solution after 200 s. (*B*, *D*, and *F*) Corresponding representative current-voltage relationships were taken from voltage ramps for a 10 mM Ca^{2+} containing bath solutions as well as a Cs^{+}-DVF solution for (*A*, *C*, and *E*). (*G*) Representative current-voltage relationships in a Na^{+}-DVF solution for Stim1 and Orai3-E85D-E89D, as well as a co-expression with Orai1 or Orai3. (*H*) Summary of reversal potentials in a Ca^{2+} and Na^{+}-DVF solution, decrease (↓) or increase (↑) of inward currents when switching from Ca^{2+} to Cs^{+}-DVF solution, and calculated permeability ratios $P_{Cs/Na}$ for Stim1 and Orai3-E85D-E89D as well as a co-expressed with Orai1 or Orai3.

thereby generating a reduced barrier for Cs^{+} flux. Therefore in a heteromeric Orai1/Orai3 channel outward currents are significantly increased in comparison to homomeric Orai channels. Consistently other selectivity properties are also altered, like Na^{+} to Cs^{+} permeability. It is likely that also Orai2, with a glutamate and glutamines at similar sites, in a heteromeric channel with either Orai1 or/and Orai3 will widen the repertoire of pore properties.

It is important to stress that all of our results were obtained from overexpressed Orai1/Orai3/Stim1 in HEK293 cells. Native Orai1 and Orai3 proteins are co-expressed in hepatocytes (18) and human airway smooth muscle cells (19), and SOC entry was reduced by both Orai1 and Orai3 RNA interference. As there is no clear evidence as yet in the literature that native Orai proteins at native levels of expression form such heteromeric channels, our report may direct research into this area. The here-discovered features of Orai1/Orai3 heteromers with diminished Ca^{2+} selectivity, increased Cs^{+} permeability, and unique inactivation profile will help to enlighten endogenous heteromeric Orai1/Orai3 channel formation in these native cells.

Materials and Methods

Molecular Cloning and Mutagenesis. Human pECFP-C1 and pEYFP-C1 Orai1 (Orai1; Accession number NM_032790) kindly provided by A. Rao's lab, Harvard Medical School, USA and Orai3 (Orai3; Accession number NM_152288) kindly provided by L. Birnbaumer, National Institute of Environmental Health Sciences, National Institutes of Health, USA were subcloned as previously described (5, 23). For the generation of the E85D-, E89D-mutants and the E85D-E89D double-mutant, pEYFP-C1 Orai3 was used as a template and suitable primers were chosen to exchange the corresponding codon from GAG (E) to GAT (D) using the QuikChange XL site directed mutagenesis kit (Stratagene). Orai3-Orai1 tandem was cloned via SOEing into pcDNA3.1V5-His/TOPO (Invitrogen) and via internal restriction sites *Bam*HI and *Xba*I into pECFP-C1 and pEYFP-C1; no linker was introduced. Human STIM1 (STIM1; Accession number: NM_003156) N-terminally ECFP-tagged was kindly provided by T. Meyer's lab, Stanford University, USA. Using a custom made mCherry vector (peGFPN-3 as backbone), Stim1 was subcloned from pcDNA3.1/V5-His TOPO via *Kpn*I and *Apa*I restriction sites.

Whole-Cell Recordings. Cells transfected (Transfectin, Bio-Rad) with Orai and Stim constructs were identified by CFP-/YFP-/Cherry-fluorescence. Electrophysiological experiments were performed at 21–25 °C, using the patch-clamp technique in whole-cell recording configurations. An Ag/AgCl electrode in combination with a 3 M KCl-filled agar bridge was used as reference electrode. For Stim1 and Orai1/Orai3 mediated currents voltage ramps were applied every 5 s from a holding potential of 0mV, covering a range of −90 to 90 mV over 1 s. The internal pipette solution designed for passive store depletion of Orai-derived currents contained (in mM): 145 Cs methane sulfonate, 8 NaCl, 3.5 $MgCl_2$, 10 HEPES, and 10 EGTA, pH 7.2. Standard extracellular solution consisted of 145 NaCl, 5 CsCl, 1 $MgCl_2$, 10 HEPES, 10 glucose, and 10 $CaCl_2$, pH 7.4. DVF solution included 150 CsCl, 10 HEPES, 10 glucose, and 10 EDTA. Where indicated, 150 CsCl was substituted by 150 NaCl. In Fig. 2g bath solution included in [mM]: 140 NaCl, 10 TEACl, 1 $MgCl_2$, 10 HEPES, 10 Glucose, and 10 $CaCl_2$. Where indicated, 140 NaCl was substituted by 140 TEACl. Applied potentials were corrected for a liquid junction of +12 mV resulting from a Cl^{-} based bath solution and a sulfonate based pipette solution. All currents are leak-subtracted either by subtracting the initial voltage ramps obtained shortly following break-in with no visible current activation or the remaining currents after 10 μM La^{3+} application at the end of the experiment both yielding identical results. All substances were purchased from Sigma-Aldrich.

Confocal FRET Microscopy. Confocal FRET microscopy was performed similarly as in (36). In brief, a QLC100 Real-Time Confocal System (VisiTech Int.) was used for recording fluorescence images connected to two Photometrics CoolSNAPHQ monochrome cameras (Roper Scientific) and a dual port adapter (dichroic: 505lp; cyan emission filter: 485/30; yellow emission filter: 535/50; Chroma Technology Corp.). This system was attached to an Axiovert 200M microscope (Zeiss) in conjunction with an argon ion multiwavelength (457, 488, 514 nm) laser (Spectra

Physics). The wavelengths were selected by an Acousto Optical Tuneable Filter (VisiTech Int.). MetaMorph 5.0 software (Universal Imaging Corp.) was used to acquire images and to control the confocal system. Illumination times of about 900–1,500 ms were typically used for CFP, FRET, and YFP images that were consecutively recorded with a minimum delay. Before the calculation the images had to be corrected due to cross-talk as well as cross-excitation. For this, the appropriate crosstalk calibration factors were determined for each of the constructs on the day the FRET experiments were performed. The corrected FRET image (N_{FRET}) was calculated on a pixel-to-pixel basis after background subtraction and threshold determination using custom-made software (37) integrated in MatLab 7.0.4 according to the method published by (38). The local ratio between CFP and YFP might vary due to different localizations of diverse protein constructs, which could lead to the calculation of false FRET values (39). Accordingly, the analysis was limited to pixels with a CFP:YFP molar ratio between 1:10 and 10:1 to yield reliable results (39).

ACKNOWLEDGMENTS. We thank S. Buchegger and B. Kenda for excellent technical assistance. M.M. was a graduate student within the PhD Program W1201 Molecular Bioanalytics from the Austrian Science Foundation (FWF). J.B. is a scholarship holder of the Austrian Academy of Sciences. I.D. is a habilitation scholarship holder of the University of Linz. I.F. is a Hertha-Firnberg scholarship holder (T442). This work was supported by Austrian Science Fund Projects P18280 (to K.G.) and P21118 and Subproject 11 within W1201 (to C.R.).

1. Parekh AB, Putney JW, Jr (2005) Store-operated calcium channels. *Physiol Rev* 85:757–810.
2. Zhang SL, et al. (2005) STIM1 is a Ca2+ sensor that activates CRAC channels and migrates from the Ca2+ store to the plasma membrane. *Nature* 437:902–905.
3. Peinelt C, et al. (2006) Amplification of CRAC current by STIM1 and CRACM1 (Orai1). *Nat Cell Biol* 8:771–773.
4. Luik RM, Wang B, Prakriya M, Wu MM, Lewis RS (2008) Oligomerization of STIM1 couples ER calcium depletion to CRAC channel activation. *Nature* 454:538–542.
5. Muik M, et al. (2008) Dynamic coupling of the putative coiled-coil domain of ORAI1 with STIM1 mediates ORAI1 channel activation. *J Biol Chem* 283:8014–8022.
6. Gwack Y, et al. (2008) Hair loss and defective T- and B-Cell function in mice lacking ORAI1. (Translated from English) *Mol Cell Biol* 28:5209–5222.
7. Vig M, et al. (2008) Defective mast cell effector functions in mice lacking the CRACM1 pore subunit of store-operated calcium release-activated calcium channels. (Translated from English) *Nat Immunol* 9:89–96.
8. Gross SA, et al. (2007) Murine ORAI2 splice variants form functional Ca2+ release-activated Ca2+ (CRAC) channels. *J Biol Chem* 282:19375–19384.
9. Gwack Y, et al. (2007) Biochemical and functional characterization of Orai proteins. *J Biol Chem* 282:16232–16243.
10. Feske S, et al. (2006) A mutation in Orai1 causes immune deficiency by abrogating CRAC channel function. *Nature* 441:179–185.
11. Yeromin AV, et al. (2006) Molecular identification of the CRAC channel by altered ion selectivity in a mutant of Orai. *Nature* 443:226–229.
12. Prakriya M, et al. (2006) Orai1 is an essential pore subunit of the CRAC channel. *Nature* 443:230–233.
13. Braun A, et al. (2008) Orai1 (CRACM1) is the platelet SOC channel and essential for pathological thrombus formation. (Translated from Eng) *Blood* 113:2056–2063.
14. Bergmeier W, et al. (2008) R93W mutation in Orai1 causes impaired calcium influx in platelets. (Translated from Eng) *Blood* 113:675–678.
15. Ong HL, et al. (2007) Dynamic assembly of TRPC1-STIM1-Orai1 ternary complex is involved in store-operated calcium influx. Evidence for similarities in store-operated and calcium release-activated calcium channel components. *J Biol Chem* 282:9105–9116.
16. Yuan JP, Zeng W, Huang GN, Worley PF, Muallem S (2007) STIM1 heteromultimerizes TRPC channels to determine their function as store-operated channels. *Nat Cell Biol* 9:636–645.
17. Liao Y, et al. (2008) Functional interactions among Orai1, TRPCs, and STIM1 suggest a STIM-regulated heteromeric Orai/TRPC model for SOCE/Icrac channels. *Proc Natl Acad Sci USA* 105:2895–2900.
18. Jones BF, Boyles RR, Hwang SY, Bird GS, Putney JW (2008) Calcium influx mechanisms underlying calcium oscillations in rat hepatocytes. *Hepatology* 48:1273–1281.
19. Peel SE, Liu B, Hall IP (2008) ORAI and store-operated calcium influx in human airway smooth muscle cells. *Am J Respir cell Mol Biol* 38:744–749.
20. Darbellay B, et al. (2008) STIM1 and Orai1-dependent store-operated calcium entry regulates human myoblast differentiation. (Translated from Eng) *J Biol Chem* 284:5370–5380.
21. Zhang SL, et al. (2008) Store-dependent and -independent modes regulating Ca2+ release-activated Ca2+ channel activity of human Orai1 and Orai3. *J Biol Chem* 283:17662–17671.
22. Lis A, et al. (2007) CRACM1, CRACM2, and CRACM3 are store-operated Ca2+ channels with distinct functional properties. *Curr Biol* 17:794–800.
23. Schindl R, et al. (2008) 2-aminoethoxydiphenyl borate alters selectivity of Orai3 channels by increasing their pore size. *J Biol Chem* 283:20261–20267.
24. Yamashita M, Navarro-Borelly L, McNally BA, Prakriya M (2007) Orai1 mutations alter ion permeation and Ca2+-dependent fast inactivation of CRAC channels: Evidence for coupling of permeation and gating. *J Gen Physiol* 130:525–540.
25. Ji W, et al. (2008) Functional stoichiometry of the unitary calcium-release-activated calcium channel. *Proc Natl Acad Sci USA* 105:13668–13673.
26. Penna A, et al. (2008) The CRAC channel consists of a tetramer formed by Stim-induced dimerization of Orai dimers. *Nature* 456:116–120.
27. Mignen O, Thompson JL, Shuttleworth TJ (2008) Both Orai1 and Orai3 are essential components of the arachidonate-regulated Ca2+-selective (ARC) channels. *J Physiol* 586:185–195.
28. Mignen O, Thompson JL, Shuttleworth TJ (2009) The molecular architecture of the arachidonate-regulated Ca2+-selective ARC channel is a pentameric assembly of Orai1 and Orai3 subunits. (Translated from Eng) *J Physiol* 587:4181–4197.
29. Hille B (1992) in *Ionic channels of excitable membranes* (Sinauer Associates, Sunderland, MA) 2nd Ed pp xiii, 337–361 p.
30. Prakriya M, Lewis RS (2002) Separation and characterization of currents through store-operated CRAC channels and Mg2+-inhibited cation (MIC) channels. *J Gen Physiol* 119:487–507.
31. Vig M, et al. (2006) CRACM1 multimers form the ion-selective pore of the CRAC channel. *Curr Biol* 16:2073–2079.
32. Scrimgeour N, Litjens T, Ma L, Barritt GJ, Rychkov GY (2009) Properties of Orai1 mediated store-operated current depend on the expression levels of STIM1 and Orai1 proteins. *J Physiol* 587:2903–2918.
33. Fierro L, Parekh AB (1999) Fast calcium-dependent inactivation of calcium release-activated calcium current (CRAC) in RBL-1 cells. *J Membr Biol* 168:9–17.
34. Hoth M, Penner R (1993) Calcium release-activated calcium current in rat mast cells. *J Physiol* 465:359–386.
35. Zweifach A, Lewis RS (1995) Rapid inactivation of depletion-activated calcium current (ICRAC) due to local calcium feedback. *J Gen Physiol* 105:209–226.
36. Singh A, et al. (2006) C-terminal modulator controls Ca2+-dependent gating of Ca(v)1.4 L-type Ca2+ channels. *Nat Neurosci* 9:1108–1116.
37. Derler I, et al. (2006) Dynamic but not constitutive association of calmodulin with rat TRPV6 channels enables fine tuning of Ca2+-dependent inactivation. *J Physiol* 577:31–44.
38. Xia Z, Liu Y (2001) Reliable and global measurement of fluorescence resonance energy transfer using fluorescence microscopes. *Biophys J* 81:2395–2402.
39. Berney C, Danuser G (2003) FRET or no FRET: A quantitative comparison. *Biophys J* 84:3992–4010.